Probing the photonic density of states using layer-by-layer self-assembly

I. Ashry,[1] B. Zhang,[1] S. V. Stoianov,[2] C. Daengngam,[2] J. R. Heflin,[2] H. D. Robinson,[2] and Y. Xu[1,*]

[1]The Bradley Department of Electrical and Computer Engineering, Virginia Tech, Blacksburg, Virginia 24061, USA

[2]Department of Physics, Virginia Tech, Blacksburg, Virginia 24061, USA

*Corresponding author: yong@vt.edu

Received January 12, 2012; revised April 10, 2012; accepted April 10, 2012; posted April 12, 2012 (Doc. ID 161426); published May 18, 2012

The process of spontaneous emission can be dramatically modified by optical microstructures and nanostructures. We have studied the modification of fluorescence dynamics using a variable thickness polymer spacer layer fabricated using layer-by-layer self-assembly with nanometer accuracy. The change in fluorescence lifetime with spacer layer thickness agrees well with theoretical predictions based on the modified photonic density of states (PDOS), and yields consistent values for the fluorophores' intrinsic fluorescence lifetime and quantum yield near a dielectric as well as a plasmonic interface. Based on this observation, we further demonstrate that self-assembled fluorophores can be used to probe the modified PDOS near optical microstructures and nanostructures.

OCIS codes: 300.6500, 160.2540, 310.0310.

It is well known that an optical microstructure or nanostructure can have a dramatic impact on the process of spontaneous emission in its vicinity. For example, significant enhancement or inhibition of spontaneous emission can be realized using structures such as photonic crystals [1,2], high Q cavities [3], plasmonic nanostructures [4,5], dielectric random media [6], and metamaterials [7]. By taking advantage of the Purcell effect [8], it is also possible to engineer spontaneous emission to realize devices such as single photon sources [9] and thresholdless lasers [10].

A fluorophore's spontaneous emission rate is controlled by vacuum field fluctuations and is proportional to the photonic density of states (PDOS) [11,12]. To characterize the modified PDOS, one can vary the distance between a fluorophore and underlying optical structures and monitor the changes in fluorescence dynamics. Previously, this distance has been controlled with methods such as Langmuir-Blodgett films [13], thermal evaporation of a dielectric thin film [14], near-field scanning [15], or layer-by-layer (LbL) assembly [16]. In this letter, we use LbL assembly to control the distance between the fluorophores and a planar substrate and correlate the resultant change in fluorescence dynamics with the predicted PDOS. Compared to other methods of distance control, the LbL approach has the important advantage of being capable of generating conformal films with sub-nm thickness control [17] on almost any surface with relative ease. Therefore, this method can be applied to a large variety of optical microstructures and nanostructures. Post-fabrication tuning of film thickness is also possible [18]. Unlike [16], here we demonstrate that fluorophores self-assembled on LbL films can be used to experimentally quantify the modification of PDOS. Using discrete emitters and additional nanolithography [17], it is also possible to investigate 3D PDOS modifications.

The quantification of PDOS is based on our experimental observation that the intrinsic quantum yield and fluorescence lifetime of the fluorophores are largely independent of the surrounding structures.

Our method is illustrated in Fig. 1. First, we immersed an Au coated glass slide in a 1 mM solution of mercaptohexadecanoic acid (MHDA) in ethanol (pH ~2) for 24 h to create a uniformly negatively charged surface. We then fabricated an LbL film consisting of alternating layers of poly(allylamine hydrochloride) (PAH) and poly (styrene sulfonate) (PSS) on the substrate following [16]. After obtaining the desired number of layers capped with a positively charged PAH layer, we immersed the sample in a suspension of negatively charged fluorophores, which adsorbed onto the film surface due to electrostatic interaction. On Si, the thiol layer is not required, and LbL films were assembled directly on a cleaned [19] substrate. Ellipsometry measurements yielded a film refractive index of 1.45 and a thickness of 3 nm per bilayer.

We used two types of negatively charged fluorophores: fluorescent polystyrene nanospheres from Phosphorex (emission peak at 680 nm, mean diameter 27 nm), and colloidal CdSe/ZnS core/shell quantum dots (QDs) from NN-LABS (emission peak at 621 nm, mean diameter 5 nm). To simplify the theoretical modeling, we limited the optical structures to planar Si wafers and planar 100 nm thick Au films. Figure 2 shows typical distributions of nanospheres and QDs, imaged by atomic force microscopy (AFM).

Photoluminescence from the surface-bound fluorophores was measured with time-correlated single-photon counting (Picoharp 300, PicoQuant) and a pulsed 473 nm laser diode (BDL-473-C, Becker and Hickl) as the excitation source. Figure 3 shows several representative

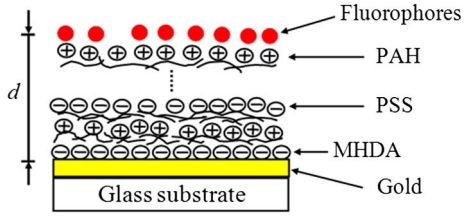

Fig. 1. (Color online) Schematic of the LbL self-assembly on a gold substrate.

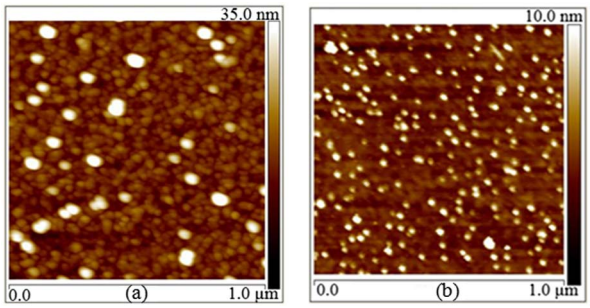

Fig. 2. (Color online) AFM images of (a) fluorescent nanospheres assembled above gold and (b) QDs assembled above Si.

examples of fluorescence decay produced by nanospheres and QDs assembled above Au and Si substrates. The decay observed in nanospheres is single exponential, but the QD fluorescence contains multiple exponential components (likely caused by randomly fluctuating charge trapping events [20]). In order to consistently evaluate fluorescence dynamics, we therefore define the average fluorescence lifetime τ as [21]

$$\tau = \int_0^\infty tI(t)\mathrm{d}t \Big/ \int_0^\infty I(t)\mathrm{d}t, \tag{1}$$

where $I(t)$ is the measured fluorescence intensity.

Electronic de-excitation can occur through fluorescent or non-fluorescent processes. Here, we define "fluorescent" emission as a process that couples a dipole to a mode described by Maxwell's equations and that therefore scales with the PDOS, even if it does not lead to far-field radiation. Fluorescent processes then include both far-field radiation and absorption into plasmon modes. With this definition, the average fluorescence lifetime τ can be found using a classical model [22]

$$\tau = \tau_0/(1 - qZ), \tag{2}$$

where the quantum yield q is the ratio between the fluorescence decay rate and the total decay rate, and τ_0 is the intrinsic fluorescence lifetime. Both q and τ_0 are defined with the fluorophore in a homogeneous medium and are intrinsic fluorophore properties. Therefore, they are independent of any dielectric or metallic structures near the fluorophores. The parameter Z in Eq. (2) describes the effect of any planar interfaces on spontaneous emission and is given by [22]

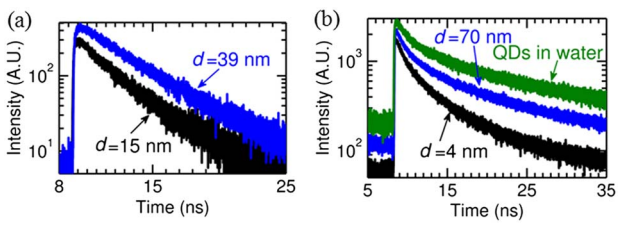

Fig. 3. (Color online) Fluorescence decay produced by (a) fluorescent nanospheres assembled above gold and (b) QDs assembled above silicon. Fluorescent lifetime measures using colloidal QDs are also given in (b).

$$Z = 1 - \frac{3}{4}\,\mathrm{Im}\int_0^\infty \mathrm{d}u\,\frac{u}{l_1}\left[\frac{F(\hat{d}, R_{12}^{\perp})F(\hat{s}, R_{13}^{\perp})}{F(\hat{d}+\hat{s}, -R_{12}^{\perp}R_{13}^{\perp})} + (1-u^2)\frac{F(\hat{d}, R_{12}^{\parallel})F(\hat{s}, R_{13}^{\parallel})}{F(\hat{d}+\hat{s}, -R_{12}^{\parallel}R_{13}^{\parallel})}\right], \tag{3}$$

where $F(x, y) = 1 + y\,\exp(-2l_1 x)$, $l_1 = -i[1 - u^2]^{1/2}$, $\hat{d} = k_1 d$, and $\hat{s} = k_1 s$. k_1 is the wave vector in the LbL film, and s represents the separation between the fluorophore and air. As shown in Fig. 1, d is the distance between the center of the fluorophore and the substrate. $R_{12}^{\perp}$ and $R_{13}^{\perp}$ refer to the s-polarization reflectivities at the film-substrate and film-air interfaces. $R_{12}^{\parallel}$ and $R_{13}^{\parallel}$ are the equivalent p polarization reflectivities. With our definition of non-fluorescent processes, Z has no impact on the non-fluorescent decay rate. Finally, all parameters in Eq. (3) are entirely determined by the planar substrate, and are independent of the fluorophores under consideration.

Figure 4 compares the predicted fluorescence lifetime with experimental data using different combinations of fluorophores and substrates. Experimental values of τ were extracted from using Eq. (1), while its standard deviation was calculated from measurements at 8 distinct locations on the same sample. For comparison with theory, we choose q and τ_0 as fitting parameters in Eq. (2) while Z was calculated from Eq. (3) using Au and Si dielectric functions from [23,24]. To account for finite nanosphere size, we assume that the fluorophores are uniformly distributed within the 27 nm sphere and obtained the average lifetime through the spatial convolution of Eq. (2). For comparison, we also considered the unconvolved case where we assume all fluorophores are at the center of the spheres. For the case of nanospheres on Au, the difference between the two cases is small (~7.9% at most). But the assumption of a uniform fluorophore distribution does improve the agreement between theory and experiment. For the case of nanospheres on silicon, assuming a uniform fluorophore distribution generates much less modification (2.2% at most) and is not shown in Fig. 4(a). Due to small QD sizes, spatial convolution was not performed in theoretical calculations. For the nanospheres, we found the quantum yield q to be 25% and 23% for the Si and Au substrates, while τ_0 was determined to be 3.8 ns and 3.84 ns,

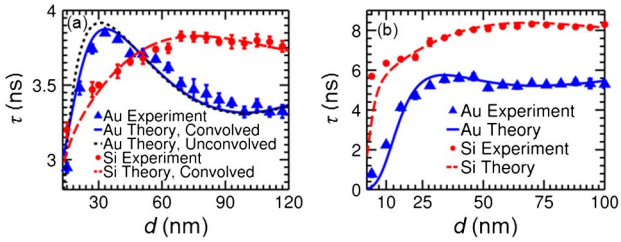

Fig. 4. (Color online) Theoretical and experimental values of fluorescence lifetime as a function of the distance d for (a) fluorescent nanospheres and (b) QDs. For nanospheres on Au, both convolved (solid blue line) and unconvolved theoretical results (dashed black line) are shown in (a). Only convolved theory is shown for nanospheres on Si.

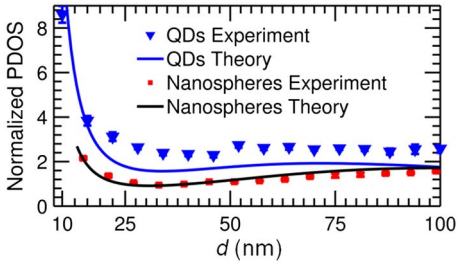

Fig. 5. (Color online) Theoretical and experimental results showing normalized PDOS as a function of the distance d for fluorescent nanospheres and QDs on gold. The theoretical PDOS refer to the values at the center of the fluorophores.

respectively. For the QDs, τ_0 was 8.2 ns for the Si wafer and 7 ns for Au film, while q was 35% for both substrates.

These results validate our expectation that for a given fluorophore and LbL film, q and τ_0 should be independent of the underlying substrate. The results also indicate that we can use the fluorophores to measure the PDOS near complex dielectric or plasmonic nanostructures. To do this, we need to first calibrate the fluorophores to find their q and τ_0 as shown above. Then, after placing the fluorophores at desired locations near the nanostructure, we can measure the modified fluorescence dynamics and extract the PDOS. To validate this approach, we used the value of q and τ_0 extracted from our convolved Si measurements. Then, the fluorescence lifetime data obtained from the Au substrate yields the plasmon-enhanced PDOS as

$$\rho(\lambda, d)/\rho_0(\lambda) = 1 - Z = 1 - [(1 - \tau_0/\tau)/q], \qquad (4)$$

where τ is the fluorescence lifetime measured on the Au substrate, $\rho(\lambda, d)$ is the PDOS in the presence of the Au substrate and $\rho_0(\lambda)$ is the PDOS in the absence of any substrate. Equation (4) was obtained from the definition of quantum yield and PDOS.

Figure 5 plots the theoretical predictions for the normalized PDOS, $\rho(\lambda, d)/\rho_0(\lambda)$, at the emission peaks of the emitters. The triangles and squares are the experimental PDOS obtained via Eq. (4). The nanosphere data reproduce the expected PDOS with high accuracy (<10% error), while the QD data show equally good agreement only for distances shorter than 20–25 nm. This is likely due to the effects of the substrates on the multi-exponential fluorescence dynamics in the QDs, which is not taken into account in our model. For many applications involving plasmonic excitations, the extreme near-field region (<20 nm) is in any case of the greatest interest.

In conclusion, we used LbL self-assembly to control the distance between fluorophores and planar optical structures to study the spontaneous emission modification induced by the change in PDOS. The results agree well with theoretical predictions. As expected, we found that a fluorophore's intrinsic quantum yield q and fluorescence lifetime τ_0 are independent of the surrounding medium. Furthermore, we can extract q and τ_0 using a planar substrate such as a Si wafer, and then use the fluorophores to quantify PDOS modification in another optical structure. For an Au substrate, the difference between theory and experiment can be less than 10%.

We thank the National Science Foundation (grants ECCS-0644488 and CBET-0756693) and the VT-MENA program for generous support.

References

1. S. Noda, M. Fujita, and T. Asano, Nat. Photon. **1**, 449 (2007).
2. G. Q. Liu, Y. B. Liao, S. J. Ma, Y. F. Shen, and Z. Q. Ye, J. Opt. Soc. Am. B **27**, 1942 (2010).
3. D. Englund, D. Fattal, E. Waks, G. Solomon, B. Zhang, T. Nakaoka, Y. Arakawa, Y. Yamamoto, and J. Vuckovic, Phys. Rev. Lett. **95**, 13904 (2005).
4. V. K. Komarala, Y. P. Rakovich, A. L. Bradley, S. J. Byrne, Y. K. Gun'ko, N. Gaponik, and A. Eychmueller, Appl. Phys. Lett. **89**, 253118 (2006).
5. C. W. Chen, C. H. Wang, C. M. Wei, and Y. F. Chen, Appl. Phys. Lett. **94**, 71906 (2009).
6. M. D. Birowosuto, S. E. Skipetrov, W. L. Vos, and A. P. Mosk, Phys. Rev. Lett. **105**, 13904 (2010).
7. Z. Jacob, J. Y. Kim, G. V. Naik, A. Boltasseva, E. E. Narimanov, and V. M. Shalaev, Appl. Phys. B **100**, 215 (2010).
8. J. M. Gerard and B. Gayral, J. Lightwave Technol. **17**, 2089 (1999).
9. W. H. Chang, W. Y. Chen, H. S. Chang, T. P. Hsieh, J. I. Chyi, and T. M. Hsu, Phys. Rev. Lett. **96**, 117401 (2006).
10. R. F. Oulton, V. J. Sorger, T. Zentgraf, R.-M. Ma, C. Gladden, L. Dai, G. Bartal, and X. Zhang, Nature **461**, 629 (2009).
11. L. Novotny and B. Hecht, *Principles of Nano-Optics* (Cambridge University, 2006).
12. W. L. Barnes, J. Mod. Opt. **45**, 661 (1998).
13. H. Kuhn, J. Chem. Phys. **53**, 101 (1970).
14. J. Y. Zhang, X. Y. Wang, and M. Xiao, Opt. Lett. **27**, 1253 (2002).
15. B. C. Buchler, T. Kalkbrenner, C. Hettich, and V. Sandoghdar, Phys. Rev. Lett. **95** (2005).
16. K. Ray, R. Badugu, and J. R. Lakowicz, Chem. Mater. **19**, 5902 (2007).
17. A. Tulpar, Z. Wang, C.-H. Jang, V. Jain, J. R. Heflin, and W. A. Ducker, Nanotech. **20** (2009).
18. K. Itano, J. Y. Choi, and M. F. Rubner, Macromolecules **38**, 3450 (2005).
19. W. Kern and D. A. Puotinen, RCA Rev. **31**, 187 (1970).
20. G. Schlegel, J. Bohnenberger, I. Potapova, and A. Mews, Phys. Rev. Lett. **88** (2002).
21. J. R. Lakowicz, *Principles of Fluorescence Spectroscopy* (Springer, 2006).
22. R. R. Chance, A. Prock, and R. Silbey, Adv. Chem. Phys. **37**, 1 (1978).
23. E. D. Palik, *Handbook of Optical Constants of Solids* Vol. **II** (Academic Press, 1985).
24. M. A. Green and M. J. Keevers, Prog. Photovoltaics **3**, 189 (1995).